Submitted in response to a **CALL FOR SCIENCE WHITE PAPERS** from the National Research Council's Committee on Astro2010: The Astronomy and Astrophysics Decadal Survey

Primary Contact: Stephan R. McCandliss, Department of Physics and Astronomy, The Johns Hopkins University, Baltimore, MD 21218, tel 410-516-5272; stephan@pha.jhu.edu

Project Lyman: Resolving the Physics Behind Reionization

Stephan R. McCandliss (jhu.edu), B-G Andersson (usra.edu), Nils Bergvall (uu.se), Luciana Bianchi (jhu.edu), Carrie Bridge (caltech.edu), Milan Bogosavljevic (caltech.edu), Seth H. Cohen (asu.edu), Jean-Michel Deharveng (oamp.fr), W. Van Dyke Dixon (jhu.edu), Harry Ferguson (stsci.edu), Peter Friedman (caltech.edu), Matthew Hayes (unige.ch), Akio Inoue (osaka-sandai.ac.jp), Ikuru Iwata (nao.ac.jp), Mary Elizabeth Kaiser (jhu.edu), Jeffrey Kruk (jhu.edu), Alexander S. Kutyrev (gsfc.nasa.gov), Claus Leitherer (stsci.edu), Gerhardt R. Meurer (jhu.edu), Jason X. Prochaska (ucolick.edu), George Sonneborn (gsfc.nasa.gov), Massimo Stiavelli (stsci.edu), Harry I. Teplitz (caltech.edu), Rogier A Windhorst (asu.edu)

Executive Summary.
The question of how and when the universe became reionized is of crucial importance for the formation of large scale structure. The relative roles of star-forming galaxies, active galactic nuclei and quasars in contributing to the metagalactic ionizing background remain uncertain. Deep quasar counts provide insights into their role, but the potentially crucial contribution from star-formation is highly uncertain due to our poor understanding of the processes that allow ionizing radiation to escape into the intergalactic medium (IGM). Direct observation at redshifts $z > 3$ of Lyman continuum (LyC) emitted below the H I ionization edge at 912 Å becomes increasingly improbable, due to the increase of intervening Ly limit systems. This favors UV and U-band optical observations in efforts to directly identify the environmental characteristics that aid LyC escape. By examining at low redshift the relationships between LyC escape and local and global parameters such as, metallicity, gas fraction, dust content, star formation history, mass, luminosity, redshift, over-density and quasar proximity, we seek to resolve the physics behind reionization. Past efforts to detect the LyC escape fraction (f_e) near $z \approx 3$ have been fruitful but observations at low redshift have been less so. We discuss the sensitivity requirements for detecting LyC leak for redshifts $0.02 < z \lesssim 3$ and $f_e \geq 0.02$ as estimated from UV luminosity functions. We find that no single instrument can work efficiently throughout the entire redshift range but that significant progress can be made at redshifts of $0.02 < z < 0.4$ with apertures as small as 0.5 – 1 meter. Apertures in excess of 2 meters will be required to work in the redshift range of $1.3 < z < 3$. The four central questions of fundamental importance to the field that can be addressed in the coming decade are:

1. What are the relative contributions of quasars, active galactic nuclei and star-forming galaxies to the metagalactic ionizing background at $z \lesssim 3$.
2. What is the relationship between f_e and the local and global galactic parameters of metallicity, gas fraction, dust content, star formation history, mass, luminosity, redshift, over-density and quasar proximity.
3. Do low-z analogs exist of the faint high-z galaxies thought to be responsible for reionization?
4. Can the escape fraction of Lyα photons (f_α) serve as a proxy for f_e?

The answer to the last question is critical for the James Webb Space Telescope (JWST) key project seeking to discover the source(s) of reionization, because Lyα is easier to detect spectroscopically than the far-UV continua of the first collapsed objects and thus will be a primary diagnostic.

Keywords: Atomic processes, Ultraviolet, Galaxies, Ionizing background, Reionization

THE ESSENTIAL ROLE OF LYC ESCAPE

Some 0.3 Myr after the Big Bang, the adiabatic expansion of the universe caused the primordial plasma of protons and electrons to cool, creating a neutral gas. Recent observations show that most of the universe has since been reionized and provide constraints to the duration of this process. Sloan Digital Sky Survey spectra of luminous high-redshift quasars have black H I Gunn-Peterson troughs, indicating a mean H I fraction of $\gtrsim 10^{-3}$ at $z \geq 6.4$ when the age of universe was ≈ 1 Gyr [1]. Evidence that reionzation started even earlier is provided by the polarization of the microwave background on large angular scales seen by the Wilkinson Microwave Anistropy Probe, which is consistent with an ionization fraction $\sim$ unity at $z \approx 11$ when the universe was ≈ 365 Myr old [2].

Complete reionization occurs when the rate of ionizing photons emitted within a recombination time exceeds the number of neutral hydrogen atoms. The duration of the reionization epoch depends on the initial mass function (IMF) of the first ionizing sources, their intrinsic photoionization rate (Q), the baryon clumping factor ($C \equiv < \rho^2 > / < \rho >^2$), and the fraction of ionizing photons that somehow manage to escape into the intergalactic medium (IGM) [3]. Of these parameters the LyC escape fraction (f_e) is the least constrained [1]. Its (often arbitrary) choice can alter conclusions regarding the nature and duty cycle of the sources thought to be responsible for initiating and sustaining reionization [4].

LyC escape plays an essential role in the formation of structure. The escape fraction of ionizing photons from galaxies is the single greatest uncertainty in estimating the intensity of the metagalactic ionizing background (MIB) over time [5]. The MIB controls the ionization state of the IGM at all epochs and may be responsible for hiding a non-trivial fraction of the baryons in the universe [c.f. 6, 7]. Ionizing radiation produced by star-forming galaxies is ultimately related to the rate of metal production by stellar nucleosynthesis [8]. The MIB intensity is a gauge of the feedback into the IGM of chemicals, mechanical energy and radiation by supernovae and stellar winds.

Ionizing radiation regulates the collapse of baryons on local and global scales [9]. Photoelectrons provide positive feedback for star formation by promoting the formation of H^-, which in turn catalyzes the production of H_2; a crucial coolant for collapse at high-z. Negative feedback occurs when photoionization heating raises the temperature and inhibits stellar collapse by increasing the Jeans mass. Photodissociation of H_2 is another form of negative radiative feedback mediated by both Lyman-Werner photons in the 912 – 1120 Å bandpass and LyC photons [10]. Whether ionizing radiation has a positive or negative effect on a collapsing body depends on the gas density, the strength of the radiation field, the source lifetime and the escape fraction of LyC photons[9, 11].

Quantification of the LyC escape fraction is at the frontier of reionization physics. The high opacity of even small column densities of H I to ionizing radiation makes the sources very faint at all epochs, but especially at redshifts $z \gtrsim 3$ [3]. Figure 1 from Inoue and Iwata [12], shows the likelihood of detecting LyC escape from star-forming galaxies becomes increasingly improbable above $z > 3$, due to a progressive increase with redshift in the number density of intervening Lyman limit and Lyα forest systems. Detections above $z > 4$, while not ruled out, will be extremely rare. This favors UV and U-band optical observations in efforts to directly identify and spatially resolve those physical environments that allow LyC to escape. By examining at low redshift the relationship between LyC escape and the local and global parameters of metallicity, gas fraction, dust content, star formation history, mass, luminosity, redshift, over-density and quasar proximity, we seek to resolve the physics behind reionization.

Project Lyman is not a single instrument. Rather it is a series of observing projects seeking evidence for f_e from $0.02 < z \lesssim 3$. Work at the higher redshifts is being carried out from the ground down to the ozone cutoff at ≈ 3100 Å ($z > 2.4$). Upper atmosphere balloons could shorten the cutoff by a few 100 Å, but it is from wide field surveys in space where the largest gains are to be made. We find a 10- to 100-fold improvement in sensitivity is possible for instruments with apertures as small as 0.5 - 1 m, perhaps launched by low cost orbital sounding rockets, which focus on spectroscopic detections of f_e at $0.02 < z < 0.4$. Sensitivity improvements will be even higher for mid-sized apertures in the 1 - 2 m range, launched from Explorer class vehicles, for work at $0.4 < z < 1.3$. Measurements from $1.3 < z < 2.4$ are extremely challenging, requiring apertures in excess of 2 m to overcome the zodiacal light background.

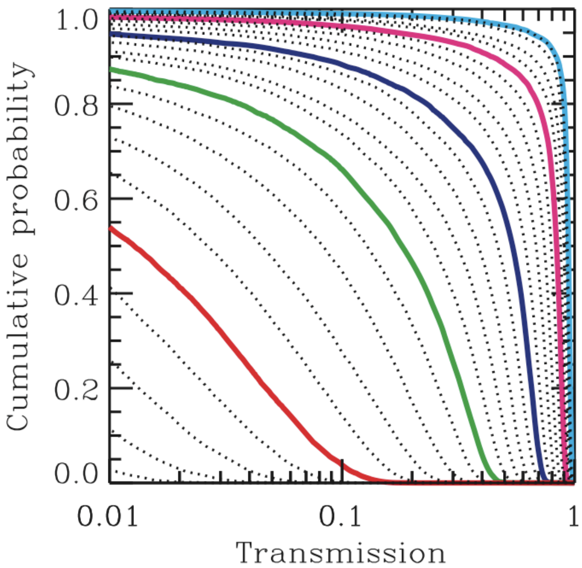

FIGURE 1. The results of a Monte Carlo [12] showing the effects of intergalactic absorption by Lyman limit systems on the transmission of LyC photons. The graph depicts the cumulative probability of having a line-of-sight transmission greater than that shown on the axis for LyC photons emitted between (880 – 910 Å). The light blue, magenta, dark blue, green and red are contours for the redshifts $z = 1, 2, 3, 4$ and 5 respectively. At $z = 4$, the probability of having a transmission of greater than 30% is 0.2

SOURCE(S) OF REIONIZATION AND THE MIB

The fundamental question is, how did the universe come to be reionized and how long did it take? Current thinking posits that LyC escape from the smallest galaxies powers reionization at $z \approx 6$, since quasars are too few in number to sustain reionization [3, 13, 14]. However, this conclusion depends on an extrapolation of the slope at the faint end of the galaxy luminosity function (LF, $-1.6 \leq \alpha \leq -2.0$), the faint end luminosity cutoff, the clumping factor ($20 < C < 45$) and $f_e \sim 0.1 - 0.2$.

The sensitivity of this conclusion to the faint end slope and the role played by the clumping factor and f_e is illustrated in Figure 2 taken from Yan and Windhorst [14]. On the left, the LFs for quasars and galaxies are displayed for a redshift of $z = 6$. Two extreme faint end slopes are shown for the galaxies (-1.6, -2.0) and for the quasars (-1.6, -2.6). On the right, two panels show the cumulative reionizing photon production rate for quasars and galaxies at a redshift of $z = 6$ and for galaxies alone at $z = 7$. Horizontal lines drawn at the top of each panel mark the critical production rate required to keep the universe fully ionized for clumping factors of 20, 30, 45 (higher clumping factors require more photon production to overcoming clump self-shielding) and assuming $f_e = 0.1$.

The figures show that at $z = 6$ the faintest galaxies dominate the LyC production and are more likely than quasars to maintain the universe in a fully ionized state. The case becomes less certain at $z = 7$ where it has been found that maintaining reionization requires either a "top heavy" IMF or escape fractions $0.3 \lesssim f_e \lesssim 0.8$, assuming $20 < C < 45$ [15, 16]. It may be that there are not enough star-forming galaxies early on to initiate reionization [17] and that mini-quasars might be involved [18]. There are also indications that the initiation of reionization above $z = 7$ may require a "hard" spectral energy distribution (SED) more characteristic of quasars [17].

Moreover, since black holes reside in the nuclei of most if not all quiescent galaxies [19, 20], it is perhaps simplistic to characterize reionization as a process caused by either quasars with $f_e = 1$ or star-forming galaxies with $f_e < 1$. Some fraction of quasars exhibit a break at the Lyman edge likely due to obscuration by host galaxies[21, 22]. The central engines of active galactic nuclei (AGN) have intermittent duty cycles, so the effects of previous AGN activity within an apparently dormant galactic environment may reduce, for a time, the local H I density aiding LyC escape. A quasar in close proximity to star-forming galaxies could produce a similar effect. Such considerations become increasingly important as the MIB budget moves from one dominated by star-forming galaxies near $z \sim 6$ to one with a quasar contribution that peaks at $z \sim 2$ [23]. Wide-field observation of f_e from objects in extended cluster environments can be used to map out the relative contribution of galaxies, AGN and quasars to the MIB in the local universe and provide a means assess its spatial uniformity in the redshift range $z \lesssim 2.3$, which cannot be probed by the ratio of He II/H I Lyα forest lines [22].

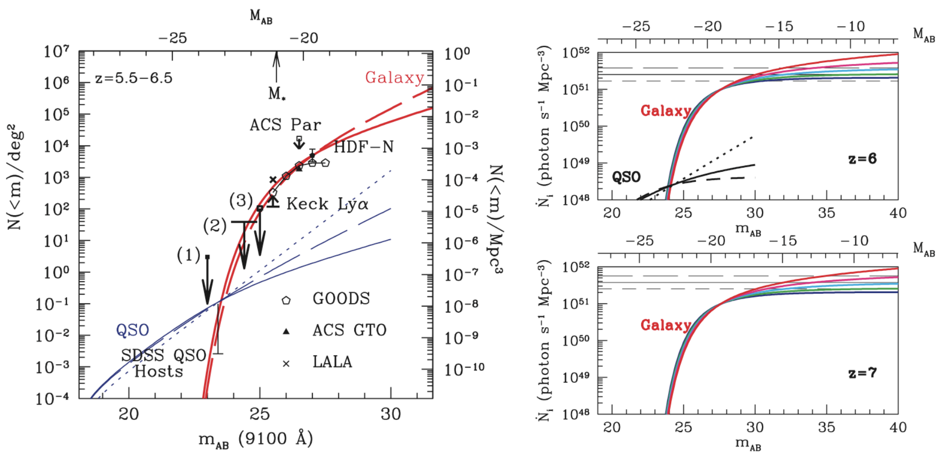

FIGURE 2. Left – LFs for quasars and galaxies at $z = 6$. Right – Reionizing photon production rate for quasars and galaxies at a redshift of $z = 6$ and for galaxies alone at $z = 7$. The production rate required to maintain a fully ionized universe for clumping factors of 20, 30 and 40 are indicated at the top of each graph. Higher clumping factors require more photon production. See [14] for details.

LYC AND LYα ESCAPE: ENVIRONMENTS, ANALOGS AND PROXY PROSPECTS

Reionization appears to require LyC leakage from galaxies with $f_e \sim 0.1$, but how LyC and Lyα escape from galaxies is somewhat mysterious. Most star-forming galaxies have mean H I columns greater than damped Lyα systems (DLA) (see Figure 3). The optical depth at the Lyman edge for DLAs is $\tau_{\lambda<912} > N_{HI}$ 6.3 x 10^{-18} $(\lambda/912)^3$ = 1260 $(\lambda/912)^3$, while at the line core of Lyα the optical depth is, $\tau_{Ly\alpha} = N_{HI}$ 6.3 x 10^{-14} = 1.26×10^7 (for V_{dop} = 12 km s^{-1}). Escape from such large mean optical depths requires that the interstellar medium (ISM) be highly inhomogeneous. The escape of Lyα (f_α) is aided by velocity gradients and the presence of multi-phase media [24, 25, 26, 27]. Similarly, LyC escape is thought to result from galaxy porosity, low neutral density, high ionization voids, chimneys created by supernovae or the integrated winds from stellar clusters [28],

In the following section we discuss how the escape fraction at $z \sim 3$ appears to be higher than at low z. Perhaps this is due to a paucity of well-formed neutral disks around galaxies at earlier epochs. The combination of tidal disruption, a much higher major merger rate [29] and starburst- or AGN-driven outflow may ionize the residual gas in young star clusters and may make it easier for the LyC emission from star formation to exceed the recombination rate [30]. At lower redshifts ($0 \le z \le 1.5$), giant H I disks have begun to settle and outflows are significantly smaller, resulting in lower f_e due to the relatively high density of H I surrounding H II regions. Nevertheless, we expect a trend whereby metal-poor dwarfs and irregulars have higher f_e than bulge and disk type galaxies because they tend to reside on the outskirts of galactic clusters and are surrounded by a more tenuous IGM with a higher ionization fraction on average. These objects may be the low-z analogs to the low mass LyC emitting objects at high-z thought to be the drivers of reionization. Furthermore, examples abound at low-z of mergers and objects with unstable disks, large scale outflows, and young star clusters embedded within clumpy, multi-phased media. In short, all the same physical conditions conducive to LyC and Lyα escape at high-z can be directly resolved in low z galaxies, up close and in depth. By characterizing f_e and f_α at low redshift in a diverse sample of galaxies, we gain insight to the physics of LyC and Lyα escape, with which we can constrain the contribution of high-z galaxies to the ionization history of the universe.

Exploring the possibility of a proxy relationship between f_e and f_α will be extremely important in the coming decade as JWST seeks to identify the source(s) responsible for initiating and sustaining reionization. The brightness of Lyα emission from the first objects is expected to be much easier to detect than their rest frame UV continuum. Consequently, JWST will probably have to rely upon observations of Lyα escape as a proxy for LyC escape. Unfortunately there is no guarantee that such a proxy relationship exists, because escaping Lyα photons are created by recombining electrons freed by the LyC photons that do not escape [31] ([Lyα $\approx (2/3)Qf_\alpha(1-f_e)exp(-\tau)$]). It is thus essential to test the proxy hypothesis at $z \lesssim 3$ by obtaining simultaneous observations of LyC and Lyα.

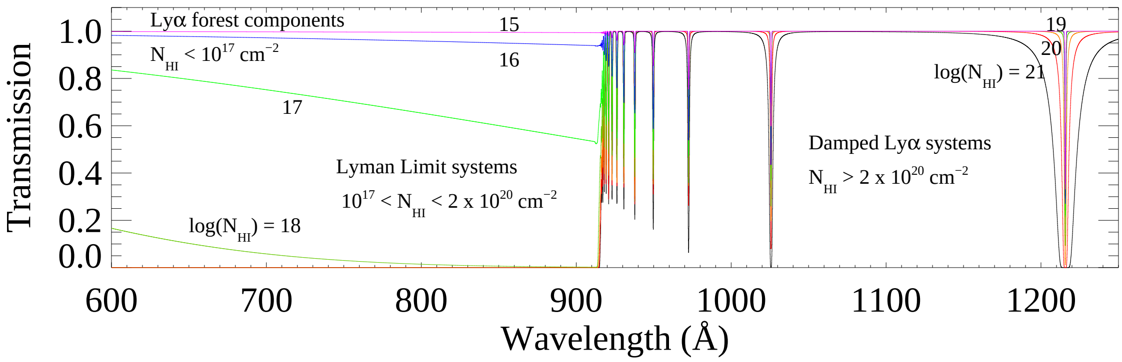

FIGURE 3. H I transmission function across the Lyman edge for damped Lyα systems, Lyman limit systems and Lyα forest components.

STATUS OF LYC ESCAPE DETECTION EFFORTS

Efforts to observe LyC emission from star-forming galaxies have returned mixed results, but hint at a trend for f_e falling towards low-z. There are no reported observations of LyC escape for $z > 3.4$. The first detection was in a composite spectral stack of 29 Lyman Break Galaxies (LBG) with a $< z >$ = 3.4 [32]. Spectroscopic detections were also reported for 2 individual LBGs at $z \sim 3$ [33]. The estimated relative escape fractions were $f_{e,rel} \sim 0.5$ [1]. In contrast, Hubble Deep Field imaging of 27 galaxies with spectroscopic redshifts $1.9 < z < 3.5$ found only an upper limit of $f_e < 0.04$ [34]. Recent narrowband imaging at $z \approx 3$ from Subaru has been more successful, finding 17 detections out of a sample of 198 with a median $f_e > 0.04$, and some objects without cospatial Lyman and far-UV continua [35].

At $1.1 < z < 1.5$, two programs [36, 37], using broadband imaging at $\approx$ 1600 Å with the solar-blind detectors on *HST* to observe 11 starburst galaxies and 21 sub-L^{*}[2] galaxies in the HDF-N and HUDF, found no detections and similar relative escape fraction limits $f_{e,rel} \lesssim 0.1$ - 0.4 and $f_{e,rel} \lesssim$ 0.08 respectively. Over a similar redshift range *GALEX* observations of 626 UV selected galaxies in the GOODS-N field find no detections with an escape limit below 1% [23]. At $z \sim 0.02$, spectroscopy from HUT and *FUSE* find only controversial detections and upper limits of $f_e < 1$ - 57% [c.f. 38, 39, 40, 5, 41, 42]. The background limits for HUT and *FUSE* were $\sim 10^{-15}$ ergs cm^{-2} s^{-1} Å^{-1} ($\equiv 1FEFU$).

Two late-breaking results reported at the January 2009 AAS continue to reinforce the trend of escape fraction decreasing with redshift. Bridge et al. [43] reported upper limits to the escape fraction of 5 to 21% from deep *HST* UV slitless spectroscopy of 14 LBG analogs in the COSMOS field with a redshift of $z = 0.7$. Their stacked limit escape fraction is $f_e < 5\%$. Bogosavljevic and Steidel [44] reported on 13 positive detections out of 120 LBG at $z = 3$, using 8 – 10 hour exposures on the Keck Low Resolution Imaging Spectrograph Blue channel. Preliminary results indicated that the escape fraction is very high ($\sim$1) and that the absorption line O I λ 877 has been found in stacked spectra below the Lyman edge. The detection frequency by Bogosavljevic and Steidel [44] (13/120) is in good agreement with the detection frequency of Iwata et al. [35] (17/198) and consistent with the non-detection frequency by Bridge et al. [43] (0/14) albeit at a lower f_e. Gamma ray burst afterglow spectroscopy indicates that roughly 5% of the sightlines from $z \sim 2$ star-forming regions are optically thin to ionizing radiation, a number comparable to these detection frequencies [45].

Spectroscopic observations hold an advantage over broad band imaging by providing the means to quantify ISM and IGM attenuation by H I using Lyman series absorption and investigating Lyα escape processes. The LyC non detections at low redshift to the few percent level for bright UV objects point to the need in future surveys for sensitivities 10 – 1000 times lower than *FUSE* to establish firm f_e limits for L^*_{uv} galaxies. A quantitative assessment of the evolving contribution of galaxies to the MIB will

[1] The ratio $f_e/f_{e,rel}$ defined to be the total dust attenuation at 1500 Å[32].
[2] L^*_{uv} is the characteristic UV luminosity of a galaxy luminosity distribution function.

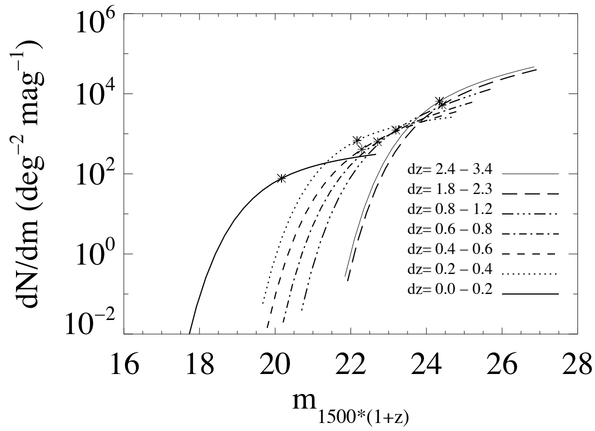

FIGURE 4. Surface densities as a function of observer's frame apparent magnitude for galaxy populations with redshifts between 0 – 0.2, 0.2 – 0.4, 0.4 – 0.6, 0.6 – 0.8, 0.8 – 1.2, 1.8 – 2.3, 2.4 – 3.4, estimated following Arnouts.[47] There are 100s – 10,000's of galaxies per square degree per magnitude with 24> $m^*_{1500(1+z)}$ > 20 for each redshift interval.

likely require spectroscopic surveys over wide angular fields to acquire the large number of observations needed for establishing LyC luminosity function [46].

LYC DETECTION REQUIREMENTS

GALEX has shown there are thousands of far-UV emitting galaxies per square degree down to its limiting magnitude $m_{FUV} \approx 25$ [48]. McCandliss et al. [49] have suggested a wide field spectroscopy survey with a two-reflection spectro/telescope, which incorporates arrays of microshutters at the prime focus along with state-of-the-art UV mirrors and detectors, is a way to efficiently search for LyC and Lyα leakage. Top level instrument designs will flow down from the sensitivity required to detect LyC escaping star-forming galaxies over the redshift interval $0.02 \lesssim z \lesssim 3$.[3] Since these are space-based observations, it is important to have a realistic estimate of the scientific potential as a function of aperture to balance mission cost against science return.

To estimate the sensitivity requirement we need the surface density of UV rest frame emitting galaxies as a function of apparent magnitude (observer frame flux) and redshift. This is shown in Figure 4, where we plot the LFs from Arnouts et al. [47] for the redshift intervals indicated in the caption. The asterisks mark the characteristic magnitude at which the LFs transition from the exponential cutoff at the bright end to the power law extension at the faint end. We convert the 1500 Å restframe characteristic magnitudes to LyC magnitudes using,

$$m^*_{900(1+z)} = m^*_{1500(1+z)} + \delta m^{1500}_{900} + \delta m_e, \tag{1}$$

with $\delta m_e = 2.5 \log f_e$ and $\delta m^{1500}_{900} = 2.5 \log\left(f_{1500}/f_{900}\right)$. Starburst99 models[50] for continuous star-formation, assuming solar metallicity, a Salpeter IMF and an upper mass cutoff of 100 $M_\odot$, yield $f_{1500}/f_{900} \approx 2$. This ratio is insensitive to age with $1.5 \lesssim f_{1500}/f_{900} \lesssim 3$ for ages 10 – 900 Gyr.

The results, as a function of z for f_e = 0.02, 0.04, 0.08, 0.16, are displayed in Figure 5 as a series of purple connect asterisks. Estimated instrumental backgrounds of high efficiency spectro/telescopes, for low redshift surveys ($z \lesssim 0.4$) in the far-UV (900 – 1800 Å) and high redshift surveys in the near-UV (1800 – 3600 Å), are shown in blue and red respectively, for apertures of 0.5, 1, and 2 m. The far-UV estimates assume SiC coated mirrors and a semi-transparent CsI photocathode, while the near-UV estimates assume MgF_2 over Al mirrors and semi-transparent GaN photocathode [51]. The lowest sensitivity point in each band was chosen to span the desired exploration space and in practice would be adjusted to fit the needs of a particular mission. In all cases the size of the slit ($36'' \times 17''$) determines the background contribution, which in the far-UV is dominated by geo-coronal Lyα and in the near-UV by

[3] The lower limit is set by the need to work at redshifts high enough to escape the H I "shadow" of the Milky-Way.

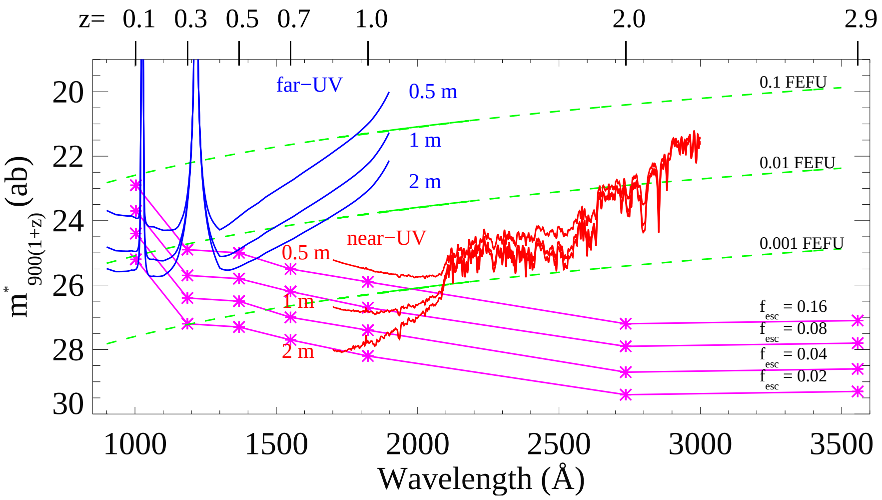

FIGURE 5. The purple connected asterisks show $m*_{900(1+z)}$ as a function of redshift for different escape fractions. Ly edge redshifts are marked at the top of the figure. Constant contours in flux units are provided (for the magnitude challenged) as green dashes marked in FEFU fractions; the background limit for *FUSE*. Estimated background limits for high efficiency UV spectro/telescopes with 0.5 m, 1 m, and 2 m apertures are overplotted in blue and red. They are dominated by geo-coronal airglow in the far-UV and zodiacal light in the near-UV. The assumed slit size was $\Omega = 36'' \times 17''$. Ω approximately 16 times smaller are possible. See [49] for details.

zodiacal light. Reducing the area of the slit reduces the background proportionally. Dashed green lines give the conversion from magnitude to flux units.

We find improvements in the background limit relative to *FUSE* of >10- to 1000-fold for 0.5 to 2 m apertures. This will enable the search for $f_e < 2\%$ in 10 – 10,000 galaxies per square degree that are brighter than L^*_{uv} in the redshift range $0.02 < z \lesssim 1.3$. Observations beyond $z > 1.3$ will be especially challenging, because of zodiacal light, requiring small angular slits on the spectrographs to limit background and apertures well in excess of 2 m.

CENTRAL QUESTIONS, PRIORITIZATION AND ENABLING TECHNOLOGIES

Understanding the mechanisms of reionization hinges on understanding how f_e changes as a function of luminosity and redshift. The answer will be important regardless of the outcome. If star-forming galaxies are found with $f_e \gtrsim 0.1$ then they become plausible sources of reionization. If not, then new physics may be required to explain reionization [52].

Four central questions of fundamental importance to the field can be addressed in the coming decade:

1. What are the relative contributions of quasars, AGN and star-forming galaxies to the MIB at $z \lesssim 3$.
2. What is the relationship between f_e and the local and global parameters of metallicity, gas fraction, dust content, star formation history, mass, luminosity, redshift, over-density and quasar proximity.
3. Do low-z analogs exist of the faint high-z galaxies thought to be responsible for reionization?
4. Can the escape fraction of Lyα photons serve as a proxy for f_e?

The answer to the last question has a high priority in the coming decade, as it is critical for the JWST key project seeking to discover the source(s) of reionization.

These questions can be most efficiently addressed using wide field spectroscopic surveys at redshifts from $0.02 < z < 3$. It is not practical to construct a single instrument to investigate f_e from $0.02 < z < 3$. Rather, the problem should be addressed using the most cost effective assets available. This means observations from the ground or balloons for the $z \sim 3$ end and space-based UV systems with 0.5 – 1 meter apertures for the lowest redshifts. Proving these technologies on sounding rocket instruments, both sub-orbital and orbital, will provide initial assessments of the science return and reduce risk and cost for more capable Explorer class missions, and beyond. Key mission-enabling technologies that will support the development of 0.°5 field-of-view, multi-object UV spectroscopy include microshutter arrays

[53], high efficiency aberration corrected dual-order gratings [54], and GaN photocathodes [51]. Future high-grasp UV telescopes sensitive enough to detect LyC leak will also easily detect the cosmic web of low surface brightness Lyα emission, providing an unambiguous beacon for emerging complexity [55].

REFERENCES

1. X. Fan, C. L. Carilli, and B. Keating, *ARA&A* **44**, 415–462 (2006).
2. D. N. Spergel et al., *ApJS* **170**, 377–408 (2007).
3. P. Madau, F. Haardt, and M. J. Rees, *ApJ* **514**, 648–659 (1999).
4. N. Y. Gnedin, *ApJ* **535**, 530–554 (2000).
5. T. M. Heckman et al., *ApJ* **558**, 56–62 (2001).
6. T. M. Tripp et al., *ApJS* **177**, 39–102 (2008).
7. C. W. Danforth, and J. M. Shull, *ApJ* **679**, 194–219 (2008).
8. N. Y. Gnedin, and J. P. Ostriker, *ApJ* **486**, 581–+ (1997).
9. M. Ricotti, N. Y. Gnedin, and J. M. Shull, *ApJ* **685**, 21–39 (2008).
10. S. R. McCandliss et al., *ApJ* **659**, 1291–1316 (2007).
11. B. Ciardi, "Feedback From the First Stars and Galaxies ...," in *AIP Conference Series: First Stars III*, edited by B. W. O'Shea, and A. Heger, 2008, vol. 990, pp. 353–363.
12. A. K. Inoue, and I. Iwata, *MNRAS* **387**, 1681–1692 (2008).
13. R. J. Bouwens et al., *ApJ* **686**, 230–250 (2008).
14. H. Yan, and R. A. Windhorst, *ApJ* **612**, L93–L96 (2004).
15. R.-R. Chary, *ApJ* **680**, 32–40 (2008).
16. A. Meiksin, *MNRAS* **356**, 596–606 (2005).
17. J. S. Bolton, and M. G. Haehnelt, *MNRAS* **382**, 325–341 (2007).
18. P. Madau et al., *ApJ* **604**, 484–494 (2004).
19. L. Ferrarese, and H. Ford, *Space Science Reviews* **116**, 523–624 (2005).
20. A. Soltan, *MNRAS* **200**, 115–122 (1982).
21. G. Kriss et al., "HUT Observations of the Lyman Limit in AGN: Implications for Unified Models," in *IAU Colloq. 159: Emission Lines in Active Galaxies*, edited by B. M. Peterson, F.-Z. Cheng, and A. S. Wilson, 1997, vol. 113, pp. 453–+.
22. J. M. Shull et al., *ApJ* **600**, 570–579 (2004).
23. L. L. Cowie, A. J. Barger, and L. Trouille, *ArXiv e-prints* (2008).
24. M. Dijkstra, Z. Haiman, and M. Spaans, *ApJ* **649**, 14–36 (2006).
25. M. Hansen, and S. P. Oh, *MNRAS* **367**, 979–1002 (2006).
26. A. Verhamme, D. Schaerer, and A. Maselli, *A&A* **460**, 397–413 (2006).
27. D. A. Neufeld, *ApJ* **370**, L85–L88 (1991).
28. A. Fujita et al., *ApJ* **599**, 50–69 (2003).
29. R. E. Ryan, S. H. Cohen, R. A. Windhorst, and J. Silk, *ApJ* **676**, 1–7 (2008).
30. J. B. Dove, and J. M. Shull, *ApJ* **430**, 222–235 (1994).
31. M. Stiavelli, S. M. Fall, and N. Panagia, *ApJ* **600**, 508–519 (2004).
32. C. C. Steidel, M. Pettini, and K. L. Adelberger, *ApJ* **546**, 665–671 (2001).
33. A. E. Shapley et al., *ApJ* **651**, 688–703 (2006).
34. A. Fernandez-Soto, K. M. Lanzetta, and H.-W. Chen, *MNRAS* **342**, 1215–1221 (2003).
35. I. Iwata et al., *ArXiv e-prints* (2008).
36. M. Malkan, W. Webb, and Q. Konopacky, *ApJ* **598**, 878–885 (2003).
37. B. Siana et al., *ApJ* **668**, 62–73 (2007).
38. C. Leitherer et al., *ApJ* **454**, L19+ (1995).
39. M. Hurwitz, P. Jelinsky, and W. V. D. Dixon, *ApJ* **481**, L31+ (1997).
40. J.-M. Deharveng et al., *A&A* **375**, 805–813 (2001).
41. N. Bergvall et al., *A&A* **448**, 513–524 (2006).
42. J. P. Grimes et al., *ApJ* **668**, 891–905 (2007).
43. C. Bridge et al., "The Lyman Continuum Escape Fraction at z 0.7," in *AAS Meeting Abstracts*, 2009, vol. 213, pp. #348.05–+.
44. M. Bogosavljevic, and C. C. Steidel, "Ionizing Radiation From Galaxies And The IGM At Z 2-3," in *AAS Meeting Abstracts*, 2009, vol. 213, pp. #362.05–+.
45. H.-W. Chen, J. X. Prochaska, and N. Y. Gnedin, *ApJ* **667**, L125–L128 (2007).
46. J.-M. Deharveng, S. Faiesse, B. Milliard, and V. Le Brun, *A&A* **325**, 1259–1263 (1997).
47. S. Arnouts et al., *ApJ* **619**, L43–L46 (2005).
48. C. K. Xu et al., *ApJ* **619**, L11–L14 (2005).
49. S. R. McCandliss et al., "Project Lyman," in *SPIE Conference*, 2008, vol. 7011, pp. 20:1–12.
50. C. Leitherer et al., *ApJS* **123**, 3–40 (1999).
51. O. Siegmund et al., *Nuclear Instruments and Methods in Physics Research A* **567**, 89–92 (2006).
52. N. Y. Gnedin, *ApJ* **673**, L1–L4 (2008).
53. A. S. Kutyrev et al., *IEEE J. Select. Topics Quantum Electron.* **10**, 652–718 (2004).
54. S. R. McCandliss et al., "FORTIS: pathfinder to the Lyman continuum," in *SPIE Conference*, 2004, vol. 5488, pp. 709–718.
55. S. R. Furlanetto et al., *ApJ* **599**, L1–L4 (2003).